PROPERTY PREDICTION WITH COUPLED MACRO-MICROMODELING AND COMPUTATIONAL THERMODYNAMICS

Jianzheng Guo, Mark T. Samonds

ESI US R&D, 5850 Waterloo Road, suite 140, Columbia, MD 21045, USA

Keywords: solidification, thermo-physical properties, mechanical properties, micro modeling

Abstract

Part of the challenge of designing a new alloy is understanding the relationships between the alloy chemistry, the processing, and the final properties of an in-service part made from that alloy. The prediction of local mechanical and thermal properties is possible, to a degree, given knowledge of the microstructure, phase fractions, and defects present in a metallic part. Multi-component micro models of solidification, coupled with macro-scale thermal and fluid flow processing conditions, including macrosegregation, have recently been coupled with computational thermodynamics in a commercial software, ProCAST, to form the basis of this type of prediction. Subsequent solid state transformations through heat treatment can also be taken into account.

Introduction

The improvement of alloy properties relies on an accurate prediction of the microstructure during solidification, defect formation, and the microstructure evolution during solid phase transformations, as might occur from heat treatment. It is critical to have accurate thermophysical properties as input for reliable simulations of the complex solidification and solid phase transformation processes. The thermo-physical properties can be calculated with the help of thermodynamic calculations of phase stability at given temperatures and compositions (CALPHAD). A comprehensive multicomponent alloy solidification model, coupled with a Gibbs free energy minimization engine and thermodynamic databases, has been developed. The computation can accurately predict microsegregation, macrosegregation, microstructure, and defects such as porosity. A back-diffusion model is integrated so that the solidification conditions, such as cooling rate, can be taken into account. A popular method for alloy strengthening is precipitation hardening. Long tempering heat treatments frequently lead to coarsening, which usually causes a lowering of the alloy yield strength and possibly its embrittlement. Therefore, it is useful to develop models to predict the kinetics of precipitation in order to control and optimize those properties.

Thermo-Physical Properties Calculation

Thermo-physical properties research is a very important part of materials science, particularly at the current times because such data is a critical input for the simulation of metals processing. There is little information about such properties for multicomponent alloys during solidification. An extensive database for the calculation of thermo-physical properties has been developed which utilizes the phase fraction information predicted with the minimization routines developed by Lukas et al. [1] and extended by Kattner et al. [2]. These properties include density, specific heat, enthalpy, latent heat, electrical conductivity and resistivity, thermal conductivity, liquid viscosity, Young's modulus, and Poisson's ratio. The thermodynamic calculation is based on the thermodynamic database from CompuTherm LLC (Madison, WI 53719 USA).

A simple pair-wise mixture model which is similar to that used to model thermodynamic excess functions in multi-component alloys is used to calculate the properties [3].

$$P = \sum_i x_i P_i + \sum_i \sum_{j>i} x_i x_j \sum_v \Omega_v (x_i - x_j)^v \qquad (1)$$

Where P is the phase property, P_i is the property of the pure element in the phase, Ω_i is a binary interaction parameter, and x_i and x_j are the mole fractions of elements i and j in that phase.

Thermal Conductivity

The thermal conductivity mainly depends on the chemical composition of an alloy. It also depends to a lesser extent on the precipitates, bulk deformation, microstructures, and other factors [4][5]. These factors can usually be ignored in the calculation of conductivity for commercial alloys.

The thermal conductivity and the electrical resistivity are related according to the Wiedeman-Franz law [6][7][8]

$$\lambda = \frac{LT}{\rho} \qquad (2)$$

where L is the Lorentz constant. $L = 2.44 \times 10^{-11} W\Omega K^{-2}$

An example of the calculated thermal conductivity of A356 is shown in Fig. 1 with experimental results for comparison. Fig. 2 shows the comparison with results from Auburn University for various alloys (http://metalcasting.auburn.edu/data/data.html). The agreement is good in general.
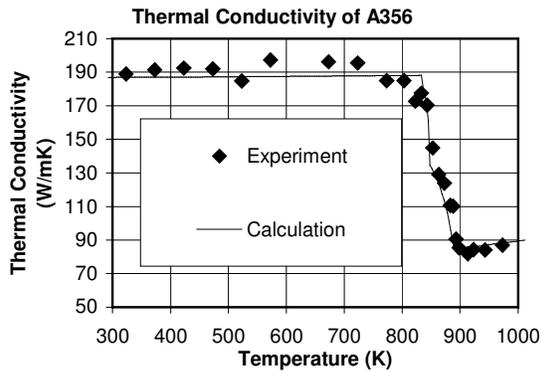

Fig. 1 Comparison between experimental and calculated thermal conductivity for A356
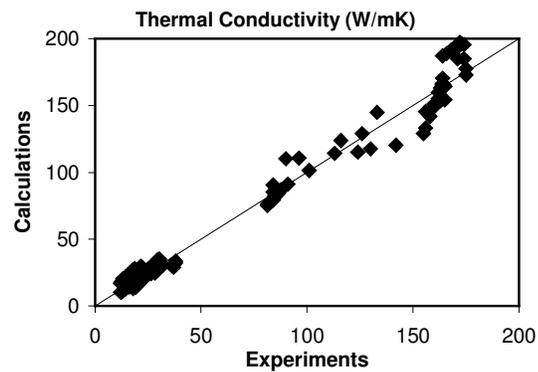
Fig. 2 Comparison between experimental and calculated thermal conductivity for different alloys

Liquid Viscosity

The liquid viscosity is a measure of resistance of the fluid to flow when subjected to an external force. The viscosity of pure liquid metal follows Andrade's relationship [9]:

$$\eta(T) = \eta_o \exp(E/RT) \qquad (3)$$

Where E is the activation energy, R is the gas constant.

Fig. 3 shows an example of the calculated liquid viscosity of an IN718 alloy using the mixture model compared with experimental results. Fig. 4 shows the comparison between experimental and calculated results for various alloys at different temperatures.
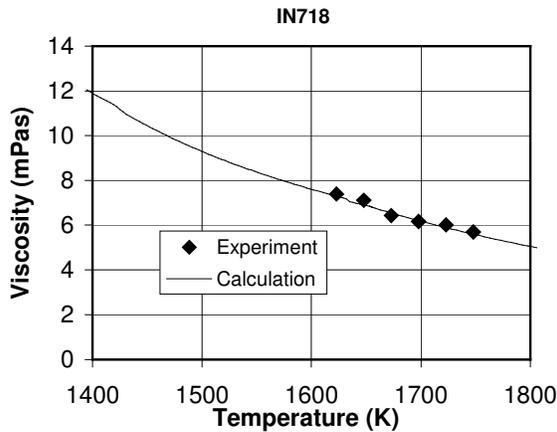

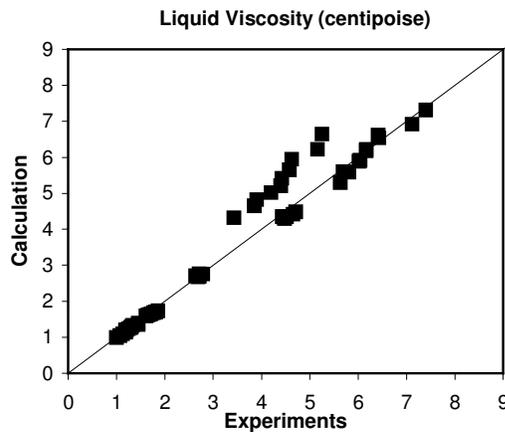Fig. 3 Comparison between experimental and calculated viscosity for IN718

Fig. 4 Comparison between experimental and calculated viscosity for different alloys

Density

A database has been developed containing molar volume and thermal volume coefficients of expansion of liquid, solid solution elements, and intermetallic phases. This is linked to the thermodynamic calculations mentioned above. The densities of the liquid and solid phases of multicomponent systems are calculated by the simple mixture model [10][11]. Fig. 5 shows plots comparing experimental values with calculations for the density of different alloys at different temperatures. Fig. 6 shows a comparison between the calculated and experimentally reported density for a Class 40 iron alloy.
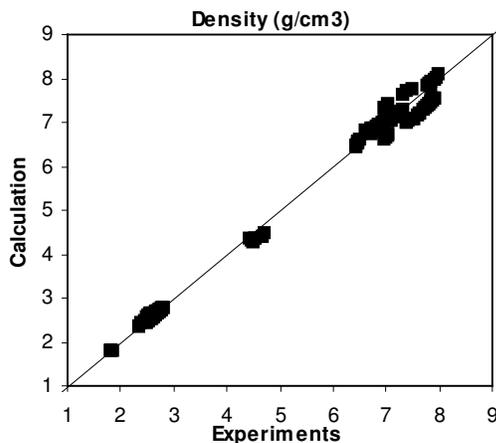

Fig. 5 Comparison between experimental and calculated density for different alloys
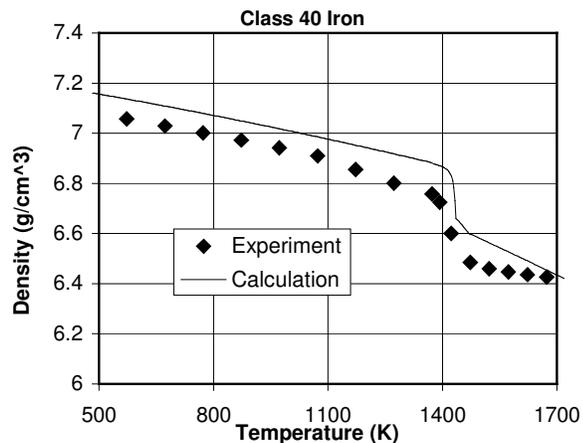
Fig. 6 Comparison between experimental and calculated density for Class 40 Iron

Solidification Simulation

Simulation technologies are applied extensively in casting industries to understand the aspects of heat transfer and fluid transport phenomena and their relationships to the microstructure, the formation of defects [14], and occasionally the final mechanical properties. The current model

includes the calculation of macrosegregation [17] and microstructure to predict multicomponent alloy casting properties. This will help foundrymen not only to minimize the problems associated with fluid flow, solidification and part distortion, by visualizing the entire casting process on the computer, but also to optimize the process by prediction of properties.

Microstructure Formation

Microstructure during solidification of alloys is a very important factor for the control of the properties and the quality of casting products [12]. Thermodynamic calculations are coupled with the macro-scale thermal and fluid flow calculations. In addition to the grain size and dendrite arm spacing, some other information can be accurately predicted, such as eutectic fraction. Fig. 7 shows the predicted results of solidification of an Al-4.9%Cu alloy compared with experiment and other model prediction results [13]. The calculated secondary dendrite arm spacing is shown in Fig. 8.
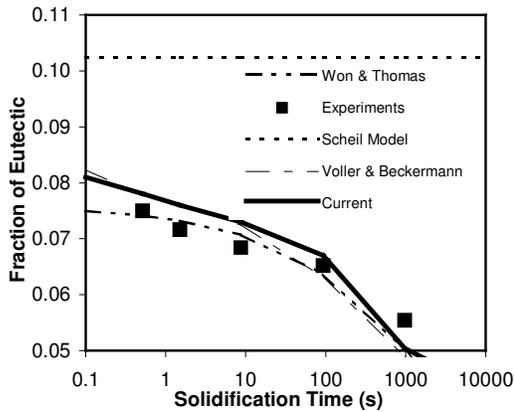
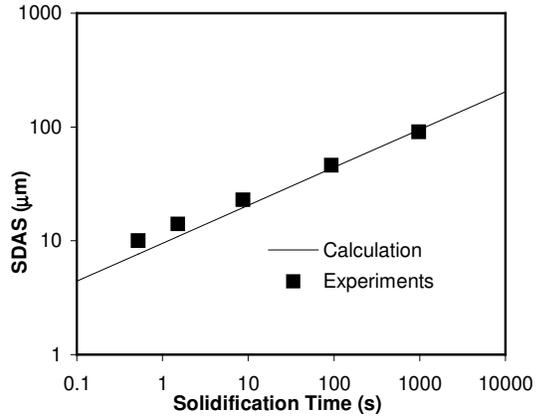Fig. 7 Eutectic fraction of Al-4.9% Cu alloy with different solidification times

Fig. 8 Secondary dendrite arm spacing

Porosity

Porosity formed in castings leads to a decrease in the mechanical properties. The porosity is a combined result of solidification shrinkage and gas evolution. Shrinkage and gas porosity can occur simultaneously when conditions are such that both exist during solidification. The liquid densities of many alloys are lower than that of the solid phase. Hence solidification shrinkage happens due to the metal contraction during the phase change. The dynamic pressure within the remaining liquid in the mushy zone at high solid fractions decreases because of the contraction and sometimes cannot be compensated by the metallostatic pressure associated with the height of the liquid metal.

The decrease of pressure lowers the solubility of gas dissolved in the liquid. Once the liquid becomes supersaturated, then bubbles can precipitate. Most liquid metals can dissolve some amount of gas. The solubility of gases in the solid phase is usually much smaller than that in the liquid phase. Normally the rejected gases during solidification do not have enough time to escape from the mushy zone into the ambient air. Being trapped within the interdendritic liquid, the gas can supersaturate the liquid and eventually precipitate as a pore if nucleation conditions are met.

The comparison of the value of percentage porosity against local solidification time and hydrogen content for an aluminum alloy between simulation and experiment is shown in Fig. 9 [14]. It shows that increasing solidification time and hydrogen contents increase considerably the percentage of porosity. Numerical simulation results give excellent agreement with the measurements of

percentage of porosity. The results also show that local solidification time and initial hydrogen content are very important factors influencing the formation of porosity.
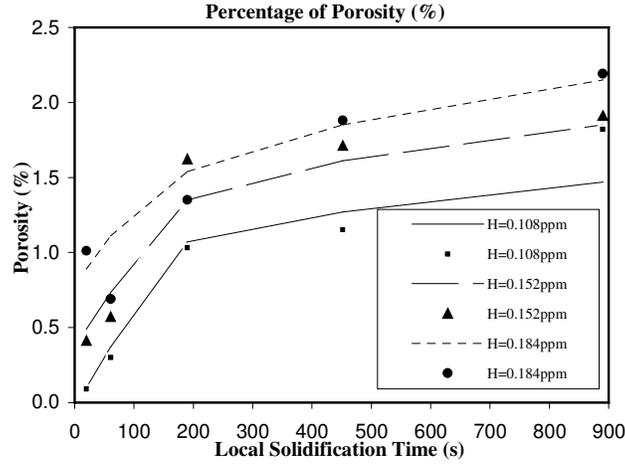

Fig. 9 The comparison between experiment (symbols) and calculation (lines)

Mechanical Properties

The ultimate goal of process modeling is to predict the final mechanical properties. There are four general methods to increase the strength of materials [15]. They are cold working, refining the grain size, solid solution strengthening, and precipitation hardening.

The standard Hall-Petch equation [20] is used to calculate the yield or proof stress of a solid solution single phase alloy.

$$\sigma_y = \sigma_o + kd^{-1/2} \tag{4}$$

Where σ_y is the yield or proof stress, σ_o is the intrinsic flow stress, k is the Hall-Petch coefficient, and d is the grain size which is calculated from the solidification micromodeling.

The high temperature strengths of many Nickel based super alloys are obtained from the ordered gamma prime (Ni$_3$Al/Ti) precipitation. A model of solid solution strengthening with the effect of gamma prime particles on dislocation motion for some Ni based alloys is presented in the following.

Precipitation Nucleation

Nucleation is the process through which the smallest stable particle of a new phase is formed. The nucleation rate is:

$$I = N\frac{kT}{h}\exp(-\frac{G^* + Q^*}{kT}) \tag{5}$$

Where N is the number density of nucleation sites, h and k are the Planck and Boltzmann constants, G^* is the activation energy required to transfer atoms across the precipitation interface.

Precipitation Growth

The diffusion rate from the diffusion field around the precipitation particle determines the precipitate growth rate. Fick's second law is applied:

$$\frac{\partial c}{\partial t} = D\nabla^2 c \qquad (6)$$

Zener [16] derived a solution to this diffusion equation for a spherical particle growth. The radius is:

$$r = \alpha(Dt)^{1/2} \qquad (7)$$

Where α is a growth parameter.

The diffusivity is calculated by:

$$D = D_o e^{(-\frac{Q}{RT})} \qquad (8)$$

Where Q is the activation energy.

The particle size and volume fraction of gamma prime precipitation can be calculated by solving the equations above.

Yield Stress:

It is easier to move the weakly coupled dislocation pairs by stress if the particle is small. The first dislocation will bow out and still keep the second dislocation straight. The yield stress will be [19]:

$$YS_1 = YS_o + M\frac{\gamma}{2b}[A(\frac{\gamma f d}{\tau})^{1/2} - f] \qquad (9)$$

Where YS_o is the yield (proof) stress due to solution hardening calculated above, M is the Taylor factor, γ is the APB (Anti-phase boundary) energy in the {111} plane, b is the Burgers vector of dislocation, d is the particle diameter calculated from the growth model, f is the volume fraction of gamma prime precipitates, and A is a numerical factor depending on the morphology of the particle. τ is the line tension of the dislocation $\tau = 1/2\mu b^2$, and μ is the shear modulus.

When the particles become large, the coupling of the dislocation can be strong. Then the yield stress can be calculated by [19]:

$$YS_2 = YS_o + 1.72M\frac{\gamma f^{1/2}}{2bd}(1.28\frac{\gamma d}{\omega\tau} - 1)^{1/2} \qquad (10)$$

Where ω is an empirical adjustable parameter.

For a given particle size, the yield stress is governed by the lower of the two value of YS_1 and YS_2.

From the formula above, it can be said that the strength of a gamma prime precipitation strengthening alloy is a complicated function of volume fraction and the size of precipitation. Fig. 10 shows the calculated solidification results of an investment casting of an IN713 alloy.
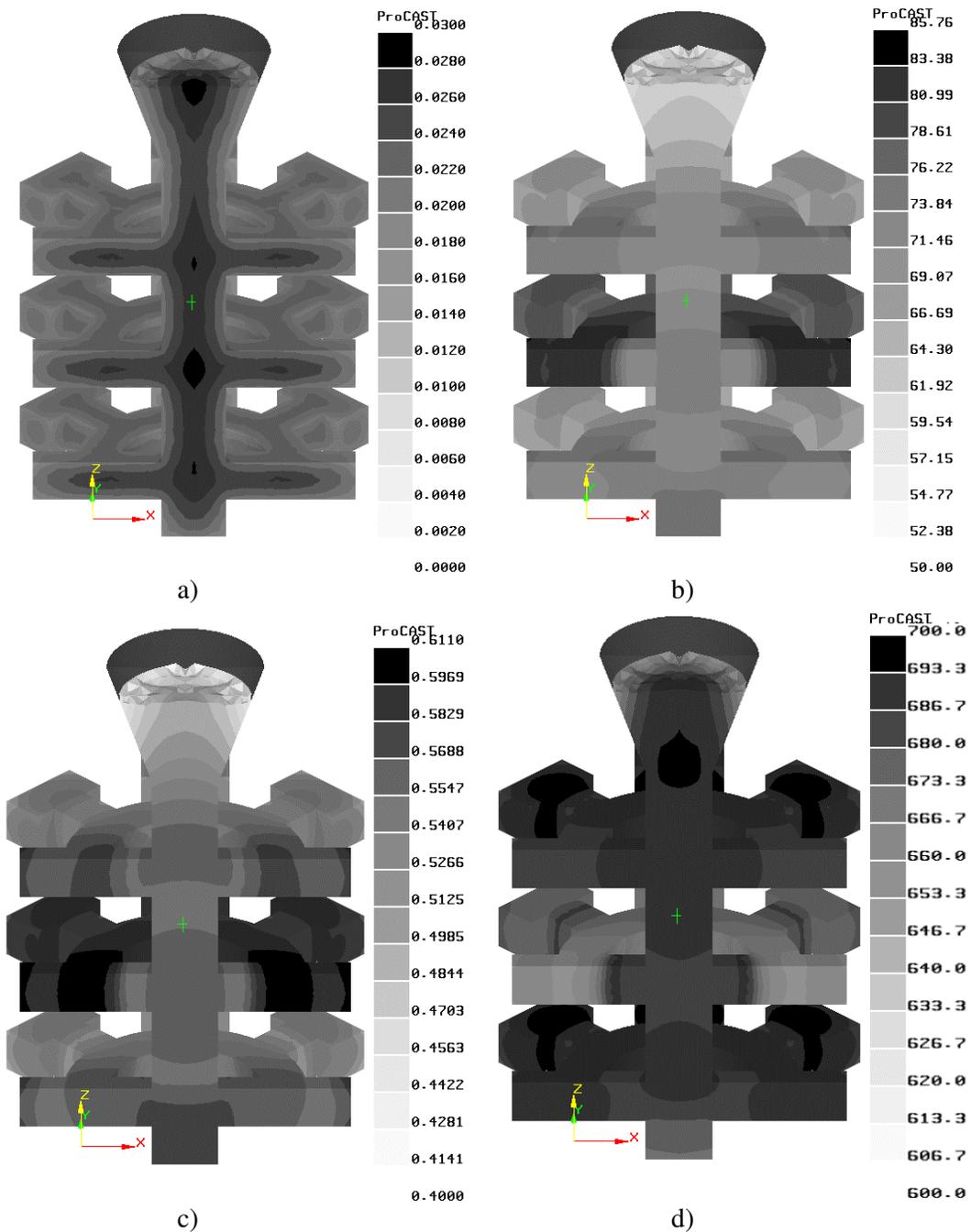

Fig. 10 Solidification of an IN713 alloy: a) Primary dendrite arm spacing (cm), b) Average gamma prime particle radius (nm), c) Volume fraction of gamma prime, and d) Yield strength (Mpa)

Conclusion

A comprehensive multicomponent alloy solidification micro-model, which is coupled with thermal-fluid macro-models, has been developed and implemented in a commercial software code, ProCAST. The thermo-physical properties can be calculated automatically through a coupled

thermodynamics calculation. The model has been validated on different alloys. The mechanical properties can be predicted by the results from the micro-modeling and by strengthening theory.

References

1. H. L. Lukas, J. Weiss, and E. Th. Henig, "Strategies for the Calculation of Phase Diagrams", CALPHAD, Vol. 6, No. 3, pp. 229-251, 1982.
2. U. R. Kattner, "The Thermodynamic Modeling of Multicomponent Phase Equilibria", JOM, Dec., pp. 14-19, 1997.
3. N. Saunders and A. P. Miodownik, CALPHAD: Calculation of Phase Diagrams A Comprehensive Guide, Pergamon,1998.
4. U. Bohnenkamp and R. Sandstrom, "Electrical Resistivity of Steel and Face-centered-cubic Iron", Journal of Applied Physics, Vol. 92, No. 8, 4402-4407, 2002.
5. B. Alkan, R. Karabulut, and B. Unal, "Electrical Resistivity of Liquid Metals and Alloys, Acta Physica Polonica A, Vol. 102, 385-400, 2002.
6. P. L. Rossiter, The Electrical Resistivity of Metals and Alloys, Cambridge University Press, 1987.
7. A. Rudajevova, M. Stanek, and P. Lukac, "Determination of Thermal Diffusivity and Thermal Conductivity of Mg-Al Alloys", Material Science and Engineering, A341, 152-157, 2003.
8. P. G. Klemens and R. K. Williams, "Thermal Conductivity of Metals and Alloys", International Metals Reviews, Vol. 31, No. 5, 197-215, 1986.
9. D. Sichen, J. Bygden, and S. Seetharaman, "A Model for Estimation of Viscosities of Complex metallic and Ionic melts", Metallurgical and Materials Transactions B, Vol. 25B, August, 519-525, 1994.
10. N. Saunders, X. Li, A. P. Miodownik, and J. P. Schille, "Modeling of the Thermo-Physical and Physical Properties for Solidification of Al-Alloys", Light Metals, 2003.
11. D. Raabe, "Computational Materials Science: The Simulation of Materials Microstructure and Properties, Wiley-VCH, 2002.
12. P. Thevoz, J. L. Desbiolles, and M. Rappaz, "Modeling of Equiaxed Microstructure Formation in Casting", *Metallurgical Tractions A*, V20A, 1989, 311-322.
13. V. R. Voller and C. Beckermann, "A Unified Model of Microsegregation and Coarsening", *Metallurgical and Materials Transactions A*, V30A, 1999, 2183-2189.
14. J. Guo, and M. T. Samonds, "Microporosity Simulations in Multicomponent Alloy Castings", Modeling of casting, Welding and Advanced Solidification Processes-X, Edited by D. M. Stefanescu, et al, Florida on May 25-30, 2003.
15. J. W. Martin, Precipitation Hardening, Woburn, MA: A division of Reed Educational and Professional Publishing Ltd, 1998.
16. P. E. Castillo, "Kinetics of Precipitation Reactions", Ph.D. thesis, University of Cambridge, 2002.
17. J. Guo, and C. Beckermann, "Three-dimensional Simulation of Freckle Formation during Binary Alloy Solidification: Effect of Mesh Spacing", Numerical heat Transfer, Part A, 44: 559-576, 2003.
18. A. J. Ardell, "An Application of the Theory of Particle Coarsening γ' Precipitate in Ni-Al Alloys", Acta Metallurgica, Vol. 16, 511-516, 1968.
19. N. Saunders, et al., "Computer Modeling of Materials Properties", *Materials Design Approaches and Experiences*, eds. J.-C. Zhoa et al (TMS: Warrendale, PA, 2001), 185.
20. E. O. Hall, Yield Point Phenomena in Metals and Alloys, (London: Macmillan, 1970).